Capability Study of Embedded Ultrasonic Transducer Microsystems for SHM Applications in Airplane Composite Structures

M. ROELLIG[1], F. SCHUBERT[1], G. LAUTENSCHLAEGER[1] ,
M. FRANKE[3], B. BOEHME[2] and N. MEYENDORF[1]

ABSTRACT

An emerging trend in modern structure design is the combination of structures and sensors in order to measure environmental conditions and to evaluate structural integrity. One possible approach of this Structural Health Monitoring (SHM) paradigm is based on ultrasonic guided waves. These elastic waves interact with damages inside the structure and the evaluation of their echo response permits damage identification and localization. Typical applications are rotor blades of wind turbines made of GFRP and aircraft components made of CFRP.

The sensor nodes consist of small piezo transducers and sensor near electronics for signal processing, power supply, and wireless communication. The high demands for lifetime and reliability of the structure are directly transferred to the electronic microsystem. The authors are working on a novel approach to embed the sensor nodes into CFRP structures. Functionality, manufacturability and reliability were experimentally investigated and supported by numerical simulations. For this purpose material characterization of the layered composite structures has been conducted to provide material data for the calculations. Finite Element Simulations help to understand the structural mechanics during simultaneous sensor embedding and CFRP-lamination and were also applied to risk estimation in terms of sensor and electronics reliability. Elastodynamic Finite Integration Technique (EFIT) was applied to study guided wave propagation inside multilayer CFRP-structures and to determine the directivity pattern of sensors laminated inside or on the surface of CFRP panels. Various sensor integration concepts were modeled to study their influence on guided wave performance and sensitivity. Finally, the numerical results were compared to experimental wave field measurements based on non-contact laser vibrometry.

MOTIVATION AND TARGET

This work is based on a SHM system, which has been developed and continuously improved for years. It operates by the ultrasonic guided wave technique to identify damages in ridged structures. Based on this separate sensor system further developments have been conducted to increase the acceptance of SHM-system as structure orientated condition

[1]Fraunhofer Institute for Non-Destructive Testing, Dresden Branch (IZFP-D)
[2]Dresden University of Technology, Electronics Packaging Laboratory (IAVT)
[3]Cotesa GmbH, Mittweida, Germany

monitoring system. In this particularly application the sensor system is supposed to be integrated in a CFRP-constructed fuselage of the new Airbus A350. The general approach is to improve the structure integration of a SHM-Sensor system by focusing the following targets:

- High efficiency of ultrasonic wave coupling and wave propagation in the CFRP-body structure,
- CFRP-Lamination process integration and
- Long lasting field operation (improve reliability).

All upper factors are equally respected during the development process.

Taking airplane structure condition, flight conditions and the conditions for the CFRP-lamination process into account several steps of development must be conducted to obtain design rules for sensor integration in CFRP-body structure.

To obtain optimal design rules for integrating the sensor in the CFRP-body structure several rounds of development will be conducted incorporating requirements for flight conditions, airplane structures and the CFRP-lamination process.

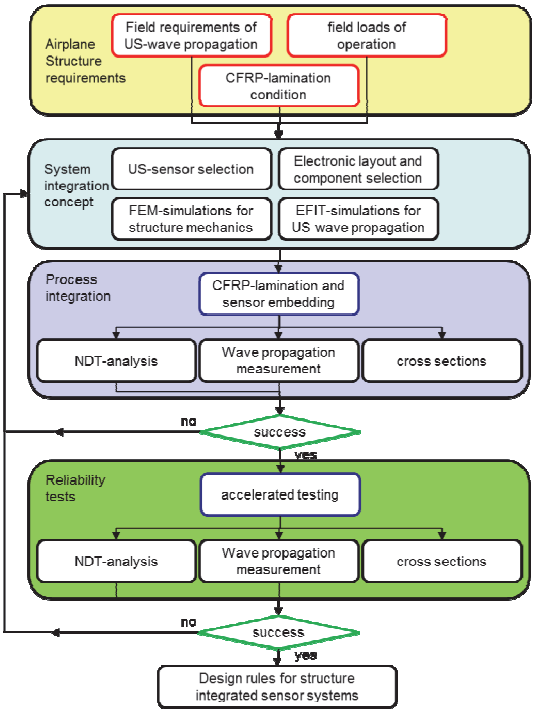

Figure 1. flow chart for sensor integration development.

State of the art technology of sensor assembly is the external attachment on the structure surface. The adhesive layer is one potential weak point in the design [1, 2], mainly due to material degradation of the a dhesive layer [3, 4]. Improved integration concepts are required.

1. INTEGRATION CONCEPTS AND LOADING CONDITIONS

At first the loading conditions for the CFRP-manufacturing process and the in-flight operation conditions were determined. The CFRP-lamination conditions were provided by the manufacturer. The in-flight conditions were provided by a test company for Airbus structure components and additionally determined from the RTCA/DO-160F standard as a guideline. Related to the airplane fuselage structure the deduced loading condition for embedded/integrated US-transducer and electronics were determined. Table 1 is an excerpt of the main factors of the loading list.

Table 1. selection of the essential loading condition on electronics and US-transducer.

#	Factor	Value Range	Occurrence
1	High Temperature	180°C for 6h	Manufacturing process
2	Pressure	7 bar	Manufacturing process
3	Temperature cycles	-55/ +85°C	In flight
4	Max. strain (uniaxial)	0,3%	In flight
5	Vibration	0,2g²/Hz	In flight
6	Moisture	til 90% r.F	In flight
7	M. shock	6-10g bei 90Hz	In flight

After having explored the system requirements, several system concepts for structure integration have been designed and iteratively improved. The concept work was strongly accompanied by simulating the resulting wave propagation characteristics and the structural loading.

Currently two approaches are favored. In concept A the US-transducer is located at the midplane (neutral plane) in the CFRP-structure. Using slim pins the transducer is electrically connected to the amplifier electronics. The electronic component is embedded between GFRP sheets, which are located on the sidewall of the CFRP-layers. The GFRP-layers are producible in the CFRP-process under the same process conditions. Additionally the GFRP and the CFRP come with the same resin matrix and therefore the material compatibility is very high. The lower GFRP-layer is an electrical insulation to the carbon fibers and conducts a strong adhesion interface to CFRP-surface. The upper GFRP-layer covers the electronics. It is compatible to organic PCB substrates like FR4 and it protects from environmental influences.

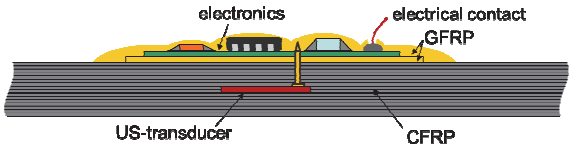

Figure 2 Concept A – US-transducer embedded in neutral plane of CFRP and electronics assembled on surface of structure.

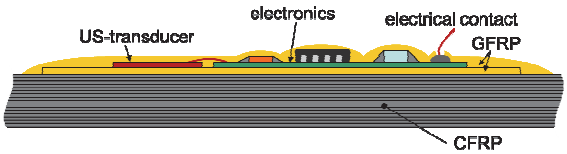

Figure 3 Concept B – US-transducer and electronics embedded in GFRP-layers and integrated on CFRP-structure surface.

Concept B consists of embedded electronics in GFRP-sheets, which are assembled on a CFRP-structure surface. Similarily, the US-transducer is located within the GFRP-covers. This approach avoids a displacement of the carbon fibers due to the embedded transducer and the vertical pin interconnections. Airplane manufacturers often object to CFRP-embedded components,since they increase the risk of destabilizing the structure. With a high probablilty concept B will lead to a higher acceptance. Furthermore, concept B provides several other advantages in the wave propagation and failure detection ability (see chapter 3).

2. MATERIAL DATA FOR CFRP-LAYERED FUSELAGE

The CFRP-Material dataset for the final fuselage of the Airbus 350 (named as CFK 977-2-34-24KIMS-194-1200) was determined before simulations were conducted. Its construction was given as 16 layer stack with CFRP prepregs consisting of Cytec 977-2-34-24KIMS. The prepreg material with its uni-directional characteristic (UD) was experimentally measured to determine the mechanical properties. The measurement standards EN ISO 527-1/4, 14129 and

14125 were applied to determine in-plane properties, which is based on the state of the plane strain. The challenge was to determine all out-of-plane components, which are required for acoustic wave propagation calculations. Additional mechanical measurements were conducted, evaluated and the resulting stiffness matrix of unidirectional CFRP-layer was extracted.

$$\begin{bmatrix} \sigma_1 \\ \sigma_2 \\ \sigma_3 \\ \tau_{23} \\ \tau_{31} \\ \tau_{21} \end{bmatrix} = \begin{bmatrix} 168{,}593159 & 3{,}827070 & 3{,}827070 & 0 & 0 & 0 \\ 3{,}827070 & 9{,}841038 & 3{,}827070 & 0 & 0 & 0 \\ 3{,}827070 & 3{,}827070 & 9{,}841038 & 0 & 0 & 0 \\ 0 & 0 & 0 & 3{,}006984 & 0 & 0 \\ 0 & 0 & 0 & 0 & 4{,}9816 & 0 \\ 0 & 0 & 0 & 0 & 0 & 4{,}9816 \end{bmatrix} \times \begin{bmatrix} \varepsilon_1 \\ \varepsilon_2 \\ \varepsilon_3 \\ \gamma_{23} \\ \gamma_{31} \\ \gamma_{21} \end{bmatrix}$$

Stiffness matrix of the uni-directional prepreg Cytec 977-2-34-24KIMS

Once the full matrix data set for the UD single layer of the CFRP core material was characterized, it was applied to the layer stack CFRP-body structure of the fuselage and the transfer of the material data into the ANSYS was conducted.

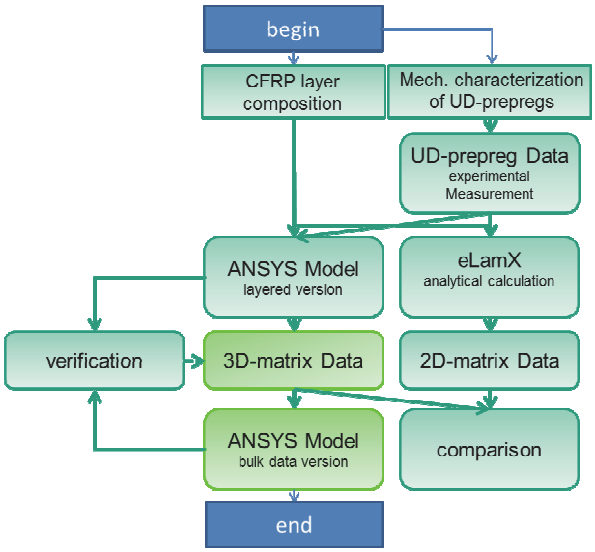

Figure 4. flow chart of the material data transfer from UD-type to the transversal isotropic data for a multi-layered fuselage.

Analytical calculations to determine the in-plane material dataset for the fuselage conditions were done by support of the eLamX-tool (Dresden University of Technology, ILR). The main purposes were the comparison with the FEM-results as plausibility check and the quantitative verification of the in-plane operating parameters.

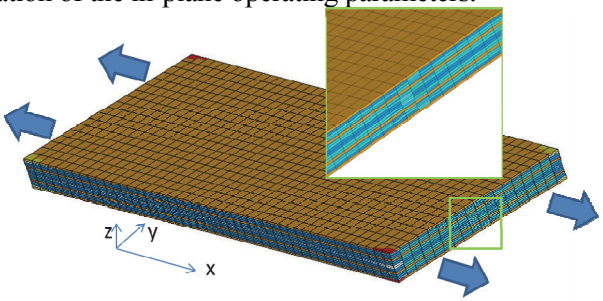

Figure 5. FEM model of a sector of the layered fuselage under tension stress.

Table 2 shows the determined dataset for the specific fuselage CFRP stack. The FEM-based values are comparable with the analytical calculated parameters. Main differences were determined in the Poisson constant vxy.

Table 2 Material data set for CFRP fuselage body Airbus 350, 16 layer, 3 mm thickness (Cytec 977-2-34-24KIMS).

	3D-matrix data (bulk)	2D-matrix data, (eLamX)	relative deviance
Exx [GPa]	60.13	63.84	5,81 %
Eyy [GPa]	60.07	63.84	5,90 %
Ezz [GPa]	9.51		
Gxy [GPa]	22.67	24.72	8,27 %
Gxz [GPa]	4.88		
Gyz [GPa]	4.72		
vxy	0.326	0.29	12,39 %
vxz	0.261		
vyz	0.269		

3. WAVE PROPAGATION AND FUNCTIONALITY INVESTIGATION

One of the key features of an embedded sensor system based on guided ultrasonic waves is the efficiency and sensitivity to detect wave excitation and detection. In a linear-elastic system both aspects are reciprocal so that the investigation of wave excitation is sufficient to characterize the sensor as a whole (including its detection capability).

In the present paper we used both numerical simulation and laser vibrometric detection to study the wave field of a piezoelectric sensor embedded in a multi-layered orthotropic CFRP laminate. The underlying material properties are described in chapter 2. The sensor was a DuraAct P876.SP1 with dimensions of 27 x 15 x 0,5 mm³ and an effective Young's modulus of 24 GPa.

For the simulation of wave propagation we used a proprietary implementation of EFIT (Elastodynamic Finite Integration Technique, [5]) which represents an explicit time-domain solver for elastodynamics. In the 3-D EFIT model the sensor was placed at different depths inside a 500 x 500 x 3 mm³ CFRP plate according to concepts A and B described in chapter 1. In this first step the electronic components in the GFRP layers were neglected. With the 3-D EFIT model we studied the effectivity for excitation of zero-order symmetric and asymmetric Lamb waves

Figure 6 illustrates the first sensor setup (concept B) in a cross-section of the 3-D model. In this case the sensor was placed on top of the plate without any additional cap strip.

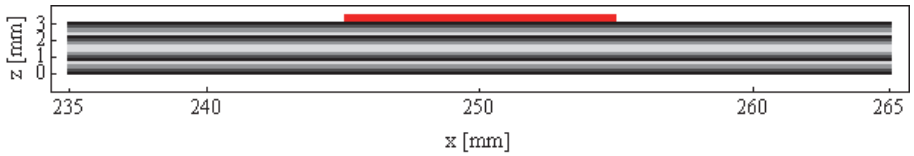

Figure 6. Cross-section of a 3-D EFIT model with a piezo-electric sensor positioned at the top surface of a 16-layer CFRP laminate (no cap strip).

The quasi-isotropic in-plane wave field caused by the pulsed excitation is shown in figure 7 at four different time points. Both the fast symmetric Lamb mode (S0) and the slower antisymmetric mode (A0) can be clearly identified.

By calculating the in-plane and out-of-plane response at a certain distance to the exciting transducer the effectivity for the S0 and A0 excitation can be determined. Figure 3 shows the results obtained in a distance of 50 mm from the center of the transducer.

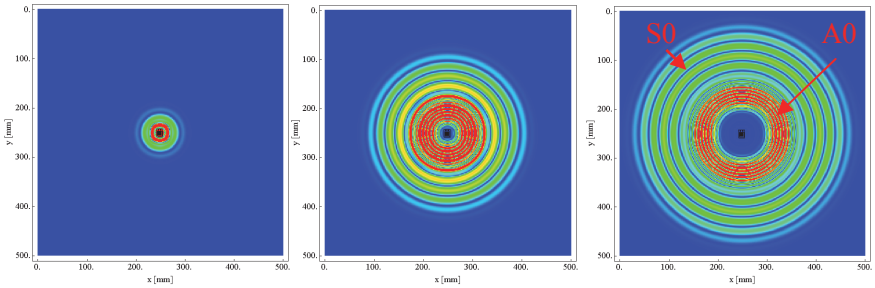

Figure 7. Numerical EFIT simulation of the Lamb wave propagation caused by pulsed excitation of the sensor shown in Figure 6. The center frequency of the input pulse amounts to 150 kHz. The pictures show the absolute value or particle velocity using a linear color scale.

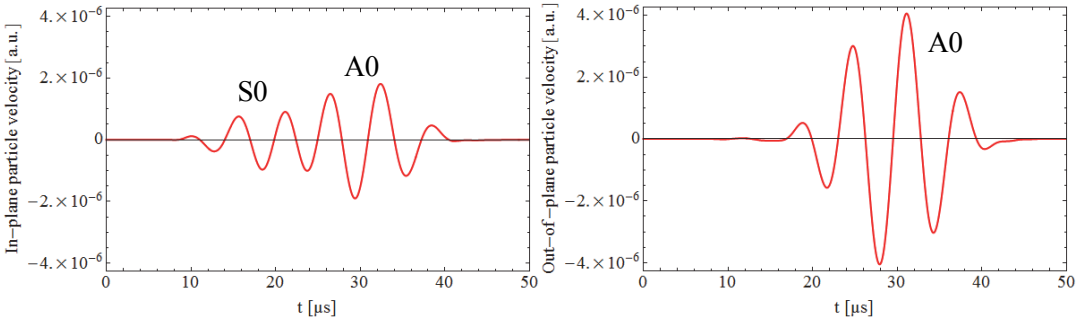

Figure 8. In-plane (left) and out-of-plane particle velocity (right) for the setup in Fig. 1 calculated at a 50 mm distance to the transducer. In this short distance S0 and A0 mode are partly superimposed so that a clear separation is not possible.

Figure 8 clearly shows that the sensor setup illustrated in Figure 6 leads to a moderately strong S0 wave but to an even stronger A0 mode. The latter is most important for the detection of delaminations and impact damage.

If we change the sensor placement to a position in the center of the laminate as shown in Figure 9, the characteristics of the excited Lamb waves also change significantly (Figure 10).

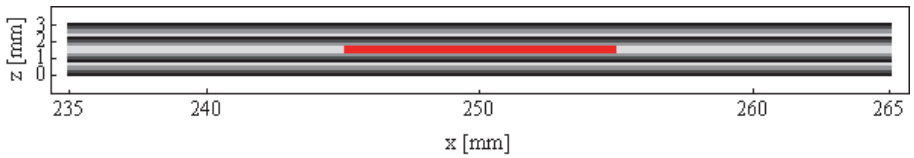

Figure 9. Cross-section of 3-D EFIT model with a piezo-electric sensor positioned at the center of a 16-layer CFRP laminate (no cap strip).

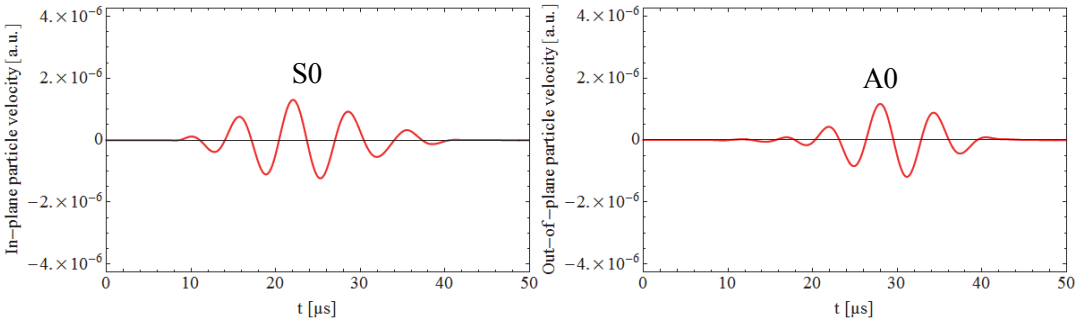

Figure 10. In-plane (left) and out-of-plane particle velocity (right) for the setup in Figure 9 calculated at a 50 mm distance to the transducer.

The second setup produced a slightly stronger S0 wave (at least in the in-plane component) but a significantly weaker A0 wave. These results indicate that for most practical applications the first sensor setup from *Figure 6* is preferred. Also for reasons of possible damage of the host structure (impact on laminate structure) the setup from *Figure 9* seems to be more problematic.

In a final step the numerical simulations were complemented by experimental measurements at a CFRP plate based on scanning laser vibrometry (Figure 11). The pictures reveal the orthotropic character of the Lamb wave field and show S0 and A0 mode as predicted by the EFIT simulations.

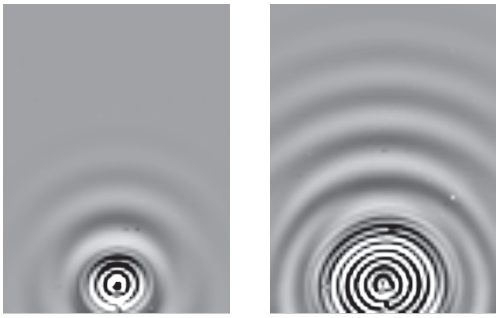

Figure 11. Time snapshots of the out-of-plane Lamb wave field across a CFRP plate measured by scanning laser vibrometry. The sensor was placed on the top surface of the plate (Figure 3). The laminate structure is identical to the one used for the EFIT simulations.

In a second step we will integrate cap strips and electronic components into the EFIT model and study their influence on the wave field characteristic. First results indicate that especially sensor concept A (*Figure 2* and *Figure 7*, respectively) is significantly affected by the additional one-sided masses.

4. TECHNOLOGY DEVELOPMENT

The concept work was assisted by the US-transducer selection and the choice of materials for the electronic packaging. The systematical evaluation of the ultrasonic transducer was conducted under considerations of processability, mechanical flexibility, ultrasonic signal strength and directional wave characteristic. Finally a polyimide package US-transducer was chosen (DuraAct-series of PiCeramics/ Invent GmbH).

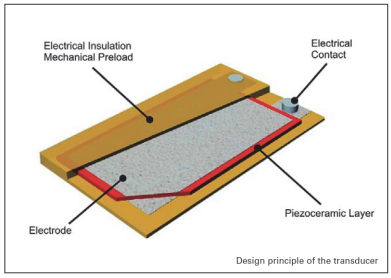

Figure 12. schematic of a PZT-transducer package from PI-ceramic [6].

The selected US-transducer was tested at T=180°C for 24h without loss of mechanical strength, electric charge and shape due to post curing effects.

The embedding technology was developed for the ultrasonic transducer and electronic components. The technology development is shown for concept B. To conduct the autoclave procedure for the CFRP lamination the system parts CFRP-layer, GFRP-layer, US-transducer and electronics are stacked. In the one step autoclave process at T=180°C and a vacuum pressure of 7 bar the stack is joined to a laminated structure (*Figure 14*).

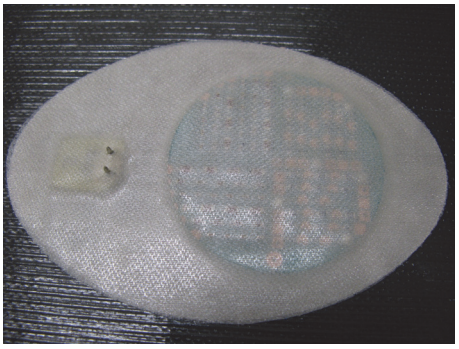

Figure 13. Preparation of differential layers to one stack before lamination; 16 layers CFRP and 4 layers GFRP inclusive the US-transducer and electronic component in between.

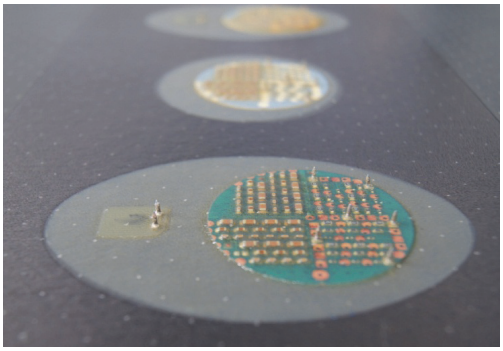

Figure 14. Embedded US-transducer and electronic component after the CFRP-lamination process.

Figure 14 shows several variations after the lamination process. The GFRP cover layers adapted very well to the surface topology caused by electronics or transducer. Additionally, fiber distortion and air enclosures were minimized.

Four indicators were/will be used to test the success of the lamination process:

- functionality tests of the US-transducer by measuring the electrical impedance,
- testing of enclosures or delamination by ultrasonic microscopy,
- tests of electrical package for e.g. damaged copper wires or solder joints by X-Ray tomography,
- functionality tests of electronic components by in circuit test.

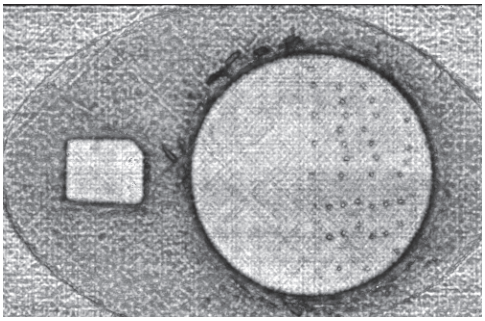

Figure 15. Quality testing after CFRP-Lamination by Ultrasonic Microscopy.

5. RELIABILITY RISK ESTIMATION BY FEM

Further FEM simulations were conducted to support the design process for embedded sensors and electronics. The loadings on an embedded microsystem needed to be estimated for the lamination process AND for the operating conditions. Selected cases were investigated as followed:

Lamination process related risks:

Cooling from 180°C to 20°C room temperature (under -2K/min) leads to induced thermo-mechanical stresses.

Case 1: embedded US-transducer package

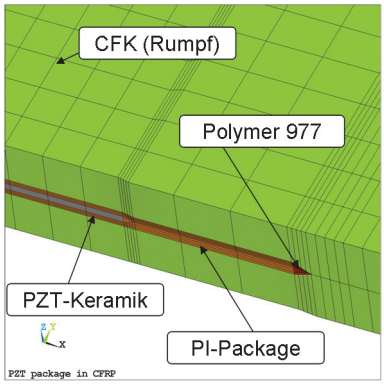

Figure 16. FEM-mesh of an embedded piezo-polymer-package in the center plane.

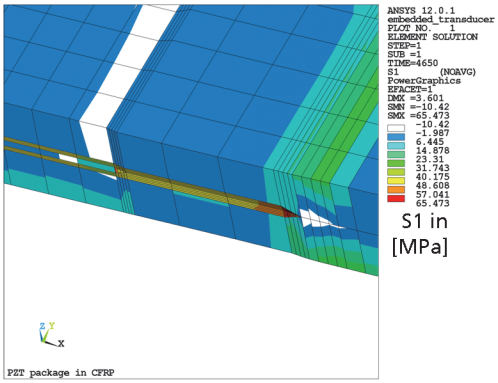

Figure 17. plot of 1st principle stress after cooling process at lamination (180°C → 20°C).

The piezo transducer package shows stronger thermal shrinkage than the CFRP-structure. Higher thermal induced stresses surround the package. At the edges the tensile stresses are highest and their orientations are out-of-plane. Stresses orientated in out-of-plane direction leads to risk of interlaminar fractures. Limits are given as 40 MPa.

Case 2: laminated electronic component

The principle selection of the material and shape of electronic carrier was investigated. The standard carrier materials Alumina-ceramic (Al_2O_3-96%) and the organic-glass fibre based PCB for high temperature application (high Tg FR4) were evaluated. The risk of high interlaminar stresses at the interface between carrier and CFRP-Surface had to be minimized. High shear stresses at the interface bring high risk of delamination and system bending.

Figure 18. sketch of embedded electronics with location of highest interlaminar stresses, comparison between different carrier materials.

At the outer edges of the electronic carrier the interlaminar stress were identified as highest. But, the selection of the organic PCB material lead to approx. 10-times lower stresses compared to Alumina. Also, round shaped carriers have to be preferred instead of rectangular substrates. The thickness of the PCB tends to lowest possible. Currently it tends to 0.5 mm.

Case 3: embedded chip-resistor on electronics

On the electronic carrier small electronic components are assembled. Following the integration concepts the electronic components are covered by GFRP layers. For demonstration purposes a ceramic chip resistor (type 0805) was used to investigate the lamination cover influences. *Figure 19* shows the FEM-mesh of an SMD-chip resistor soldered on PCB.

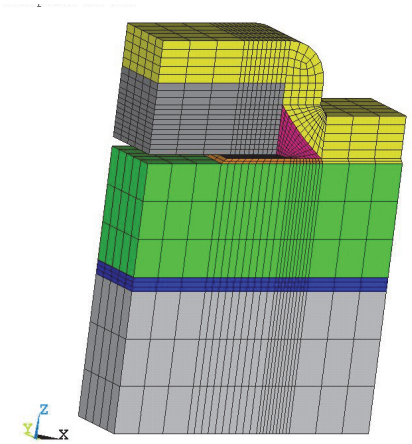

Figure 19. Mesh of an SMD chip-resistor soldered on PCB and laminated on CFRP-structure inclusive a GFRP cover layer

Again the influence of substrate material was tested. Alumina carrier induces less stresses to solder joints compared to an organic-glass fiber composite (high Tg FR4). The resulting plastic strains (creep) inside the solder joints are approx. 50% lower for the Alumina substrate than for organic-glass composites. The total creep strain in solder gap after cooling was 1%.

System operation related risks:

Environmental Operation conditions stress the total system once the sensor system is embedded in the CFRP-body structure. Once the sensor system is embedded in the CFRP-body structure the complete system is loaded by the operation conditions

Table 1 demonstrates that temperature cycles are one of the dominating loads. In electronic components temperature cycles strongly influence the mechanics. Many different materials are assembled to one system. Typically the solder joints are the weakest structure element in electronic systems. The right choice of material may extend the lifetime of the solder joints. The upper FEM-model (*Figure 19*) was loaded by a temperature shock profile from +85°/-55°C (15 min dwell time and 60 min cycle time).

First, the effect of the GFRP-cover on the creep strain at the solder joint was determined. The application of a GFRP-cover reduced the creep strain by approx. 80% compared to the non-covered electronic. This was an enormous reduction of the stresses and most likely enhances the lifetime of solder contacts significantly.

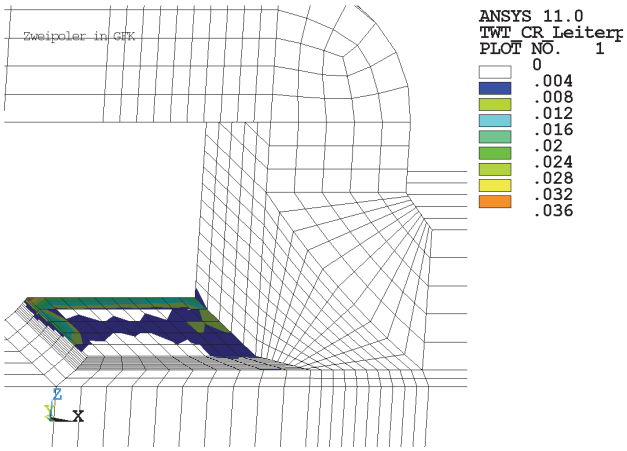

Figure 20. creep strain distribution inside a solder joint of the embedded chip-resistor (0805).

Second, the selection of Alumina as electronic carrier further improved the creep strain loading. The solder creep strain was reduced by 31% compared to organic-glass fiber substrate.

6. CONCLUSIONS

The work describes a novel embedding technology of ultrasonic transducer packages and electronic components. Practical work was supported by simulations to test functionality and reliability. From the wave propagation simulations it can be concluded that sensor concept B is superior to concept A, because it produces a significantly stronger A0 Lamb wave. This wave is essential for efficient detection of delaminations and impact damage in CFRP components. The effect of electronic components and cap strips on the excited wave field still needs to be investigated in forthcoming simulations and experiments. It is expected that these additional parts will influence the homogeneity and symmetry of the wave field to some degree.

	Integration concepts	
	A (in body)	B (surface)
Detection of delamination (A0-wave)	o	+ +
CFRP-lamination process compatibility	+	+ +
No affects to CFRP-fibers	- -	o
Alumina substrate for electronics	-	-
FR4 – substrate for electronics	+	+

The investigations on the electronic carrier have shown that alumina adapted better to the electronic components, but that it is nearly incompatible to the CFRP-structure. Interlaminar stresses prevent the use of alumina as electronic carrier.

The GFRP-cover improved the loading distribution during process cooling and temperature cycles. It reduced the mechanical strain in solder joints significantly.

ACKNOWLEDGMENTS

This project is funded by the European Regional Development Fund (EFRE) and the Free State of Saxony

REFERENCES

1. Hildebrandt, Samuel; Boehme, B.; Wolter, K.-J.; Influence of Accelerated Aging on the Acoustic Properties of a Ceramic Microsystem for Structural Health Monitoring; ESTC 2010, Berlin, 13-16 September; 2010
2. Roellig, M.; Schubert, L.; Lieske, U.; Boehme, B.; Frankenstein, B.; Meyendorf, N.; FEM assisted Development of a SHM-Piezo-Package for Damage Evaluation in Airplane Components; 11th International Conference on Thermal, Mechanical and Multi-Physics Simulation and Experiments in Micro-Electronics and Micro-Systems (EuroSimE), Bordeaux, Fr, 26.-28. April, 2010
3. Boehme, B.; Roellig, M.; Wolter, K.-J.; Moisture Induced Change of the Viskoelastic Material Properties of Adhesives for SHM Sensor Applications, 60th ECTC (IEEE); San Diego, USA, 1.-4. Juni, 2010
4. Roellig, M.;Boehme, B.; Lautenschlaeger, G.; Koehler, B.; Schubert, F.; Heinrich, F. .; Bergander, A..; Schulz, J.; Wolter, K.-J., Hentschel, D.; Franke, R.; Integration of US-based SHM Sensor System in CFRP-Airplane Structures, 4th Airportseminar; Dresden; 3-4. November; 2010

5. Schubert, F.; Numerical time-domain modeling of linear and nonlinear ultrasonic wave propagation using finite integration techniques – Theory and applications, Ultrasonics 42, 221-229, 2004.
6. DuraAct – Piezoelectric Patch Transducers for Industry and Research, www.piceramic.de

---

Contact: Dr. Mike Roellig,
Head of Department Testing and Diagnostic Systems,
mike.roellig@izfp-d.fraunhofer.de, +49(0)351 888 15 557

Dr. Frank Schubert,
Head of Department Mathematical Methods
Frank.schubert@izfp-d.fraunhofer.de , +49(0)351 888 15 523

Fraunhofer Institute for Non-destructive Testings, IZFP-D
Maria-Reiche-Str.2
01109, Dresden
Germany